Inorganic Chemistry

Article

pubs.acs.org/IC

New Aqua N-Heterocyclic Carbene Ru(II) Complexes with Two-Electron Process as Selective Epoxidation Catalysts: An Evaluation of Geometrical and Electronic Effects

Mohamed Dakkach,[†,‡] Ahmed Atlamsani,[‡] Teodor Parella,[§] Xavier Fontrodona,[†] Isabel Romero,*[,†] and Montserrat Rodríguez*[,†]

[†]Departament de Química i Serveis Tècnics de Recerca, Universitat de Girona, Campus de Montilivi, E-17071 Girona, Spain

[‡]Laboratoire des Matériaux et Systèmes Interfaciaux, Département de Chimie, Faculté des Sciences, B.P. 2121, 93000 Tétouan, Morocco

[§]Departament de Química i Servei de RMN, Universitat Autònoma de Barcelona, Cerdanyola del Vallès, E-08193 Barcelona, Spain

Supporting Information

ABSTRACT: New ruthenium complexes with general formula $[Ru^{II}(T)(CN\text{-}Me)X]^{n+}$ (X = Cl^- or H_2O; T = 2,2′:6′,2″-terpyridine, trpy, or *N*,*N*-bis(2-pyridyl)ethylamine, bpea; CN-Me = *N*-methyl-*N*′-2-pyridylimidazolium) have been prepared. The complexes obtained have been characterized in solution by spectroscopic (1D- and 2D-NMR and UV−vis) techniques, mass spectrometry, and elemental analysis. The chloro complexes have also been characterized by X-ray diffraction analysis. The redox properties of all the compounds were studied by CV revealing, for the reported Ru−OH_2 complexes, bielectronic Ru(IV/II) redox processes throughout a wide pH range. The catalytic activity of aquo complexes was evaluated in the epoxidation of olefins using PhIO as oxidant, displaying in general good yields and high selectivities for the epoxide product. The influence of electronic and geometrical factors on the spectroscopic and electrochemical properties as well as on the catalytic activity is discussed.

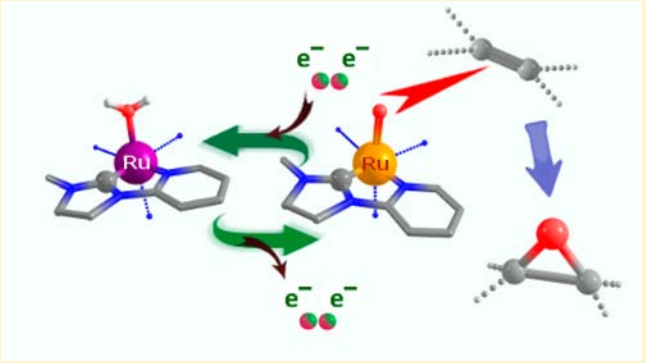

INTRODUCTION

In the past few years, N-heterocyclic carbenes (NHC) have emerged as ligated versatile building blocks for a large variety of organometallic and coordination compounds.[1,2] These ligands, in comparison to others (e.g., phosphane, amine, alkoxy, thioether, Schiff base), show a high propensity to act as excellent σ-donors and to generate stable bonds with transition metals.[3] The strong bonding metal-NHC makes complexes generally less susceptible to decomposition and increases the catalytic performance of metal complexes.[4] However, a loss of activity may be observed if the complex formed becomes too stable. To overcome this problem, the development of bifunctional ligands was considered, with the idea of combining the properties of NHC with other type of donor atoms which form not so stable bonds with the metal center (e.g., N atoms in amines), then relatively destabilizing the complexes and improving their reactivity and catalytic properties.

The Ru^{II}−H_2O complexes are of interest since the corresponding higher oxidation states can be reached within a relatively narrow potential range by sequential electron and proton loss then leading to the corresponding Ru^{III}−OH and Ru^{IV}=O species. These higher oxidation states, especially Ru^{IV}=O, are active catalysts for a variety of oxidative reactions.[5] In the chemistry of Ru^{II}−H_2O type complexes, a challenging aspect is to tune the properties of the bounded ligands so that a right combination of donor groups can lead to the disproportion of oxidation state III into Ru(II) and Ru(IV), then allowing a bielectronic Ru^{II}−OH_2 ↔ Ru^{IV}=O transformation. This would allow the occurrence of a concerted oxo-transfer mechanism in oxidation reactions catalyzed by this type of systems. This is particularly interesting in olefin epoxidation given the interest of this reaction both at an academic level and in chemical industry,[6] due to the use of epoxides as raw materials for epoxy resins, paints, surfactants, or as intermediates in organic syntheses.

We recently reported a bielectronic Ru^{II}−OH_2 complex containing two C-donor NHC rings, which constitutes the first report of a Ru−OH_2 carbenic complex studied as epoxidation catalyst.[7] The occurrence of a bielectronic (IV/II) wave in this complex improves the selectivity and avoids the *cis*/*trans* isomerization when using *cis* olefins as substrates. After that, a second report describes a new Ru catalyst containing the 2,2′:6′,2″-terpyridine (trpy) ligand together with the mono-carbene CN-Me ligand, showing that a unique NHC ring in the complex also allows the existence of a bielectronic (IV/II) wave

Received: December 31, 2012
Published: April 22, 2013

   dx.doi.org/10.1021/ic302863h | *Inorg. Chem.* 2013, 52, 5077−5087

for the Ru−OH_2 complex.[8] Given the importance of bielectronic catalysts[9] in organic synthesis, we decided to extend the study to other types of ligands in order to shed some light into the geometrical and electronic factors that can favor the disproportion of the Ru(III) oxidation state and consequently allow a 2-electron redox process in newly designed catalysts.

With all this in mind, we present here the synthesis and complete characterization of a family of Ru complexes containing the ligands displayed in Scheme 1. An analysis of the geometrical and electronic effects has been performed to rationalize their spectroscopic and electronic properties, together with the performance of the aquo complexes in the epoxidation of various olefin substrates.

Scheme 1. Ligands Used in This Work

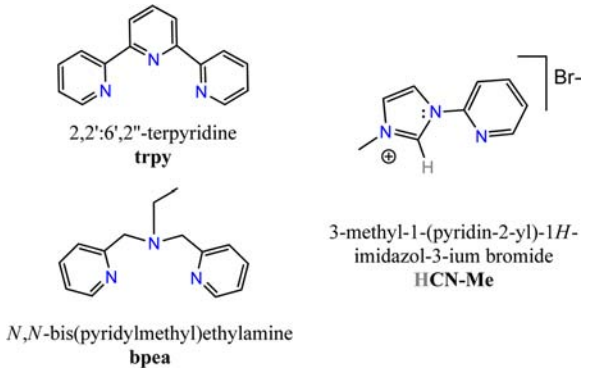

RESULTS AND DISCUSSION

Synthesis and Structure. Scheme 2 displays the synthetic strategy followed for the preparation of the whole set of complexes (the syntheses of compounds *trans*-**6** and *trans*-**7** have been described previously[8] but are included here for comparison purposes). The nomenclature *trans* or *cis* in the case of complexes **6** and **7** (containing the tridentate trpy ligand) refers to the relative position of the monodentate (Cl or H_2O) ligand with regard to the coordinating C atom of the CN-Me carbene ligand (see Scheme 3). On the other hand, the nomenclature *trans,fac* for complexes **3** and **5**, containing the facial bpea ligand, indicates the relative position of the monodentate ligand with respect to the aliphatic N atom of the tridentate bpea ligand.

The preparation of the complexes follows a similar strategy when using either bpea or trpy as tridentate ligand. A starting complex ([$Ru^{II}Cl_2$(bpea)dmso], **1**,[10] or [$RuCl_3$(trpy)], **2**[11]) is led to react with the hydrobromide form of the CN-Me ligand in presence of triethylamine and LiCl to generate the respective chloro complexes **3** or **6**. A single *trans,fac*-isomer is obtained for the bpea chloro complex **3**, whereas a mixture of *cis*- and *trans*-isomers (1:4 respectively) is attained for complex **6** containing the trpy ligand, which are separated through column cromatography. In the case of the chloro complex **3**, the analogous *trans,fac*-[RuBr(CN-Me)(bpea)]$^+$ bromo complex, *trans,fac*-**4**, has also been isolated from the reaction mixture due to the presence of the bromide counterions of the [HCN-Me]Br ligand. The formation of this side product can be avoided using 12 equiv of LiCl in the synthesis of **3**.

The coordination of the CN-Me ligand in complex **3** can potentially lead to seven different diastereoisomers (Scheme 3) including those arising from a hypothetical meridional arrangement of the bpea ligand, which has been reported previously to coordinate in such a mode thanks to its flexibility.[12] However, the synthesized complex is isolated exclusively as *trans,fac*. This can be explained in terms of (a) the kinetic stability of the meridional coordination of bpea, which is likely to be thermally converted into the thermodynamically most stable facial disposition,[12a] and (b) the occurrence of two hydrogen bonds between the monodentate chloro ligand and the H atoms in the 2-position of the pyridyl rings of bpea (depicted in orange color in Scheme 3), which can only take place in the *trans,fac* isomer and which have been shown to be determining in the isomeric ratio obtained for Ru complexes containing bpea together with N- or P-donor didentate ligands.[12c] The *trans,fac* geometry is also found in the bromo complex **4** obtained as side product (see Supporting Information for the X-ray structure of this complex).

The asymmetry of the CN-Me ligand can also lead to the formation of the *cis* and *trans* diastereoisomers in the synthesis of complex **6**, and indeed, both isomers are obtained in a 1:4 ratio, respectively. The marked preference for the *trans* isomer could be *a priori* explained by the occurrence of a H-bond in *trans*-**6**, involving the chloro ligand and the 2-pyridyl H atom of CN-Me (this is clearly manifested by its chemical shift in ^{1}H NMR, 8.10 for *cis*-**6** and 10.15 for *trans*-**6**[8]). Also, steric arguments could be invoked since, in *cis*-**6**, the methyl group of the CN-Me ligand is in close proximity to the monodentate Cl ligand. However, we described recently[13] the synthesis of a pair of analogous complexes with almost identical structure (in this case replacing the CN-Me ligand by *pypz-Me*, 2-(1-methylpyrazolyl)-pyridine), and the corresponding *trans* and *cis* isomers were yielded in a roughly 1:1 ratio. Then, neither H-bonding nor steric hindrance can explain the preferential formation of

Scheme 2. Synthetic Strategy

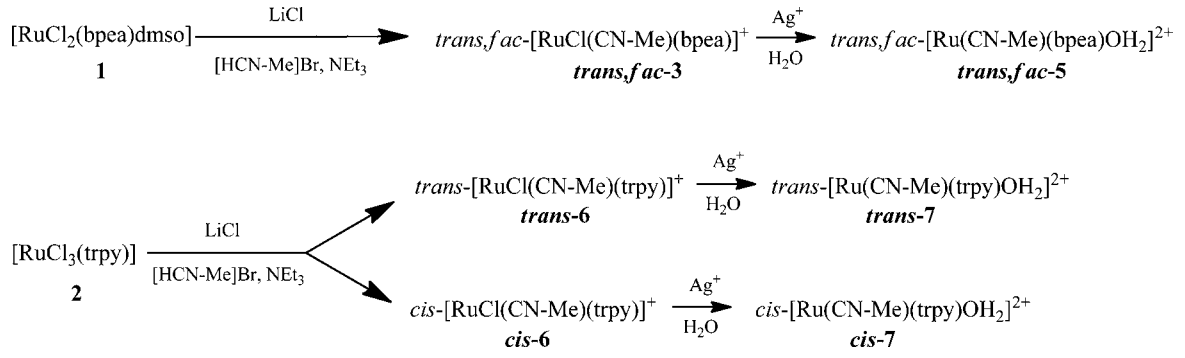

dx.doi.org/10.1021/ic302863h | Inorg. Chem. 2013, 52, 5077−5087

Scheme 3. Possible Diastereoisomers for Complexes (A) 3 and (B) 6[a]

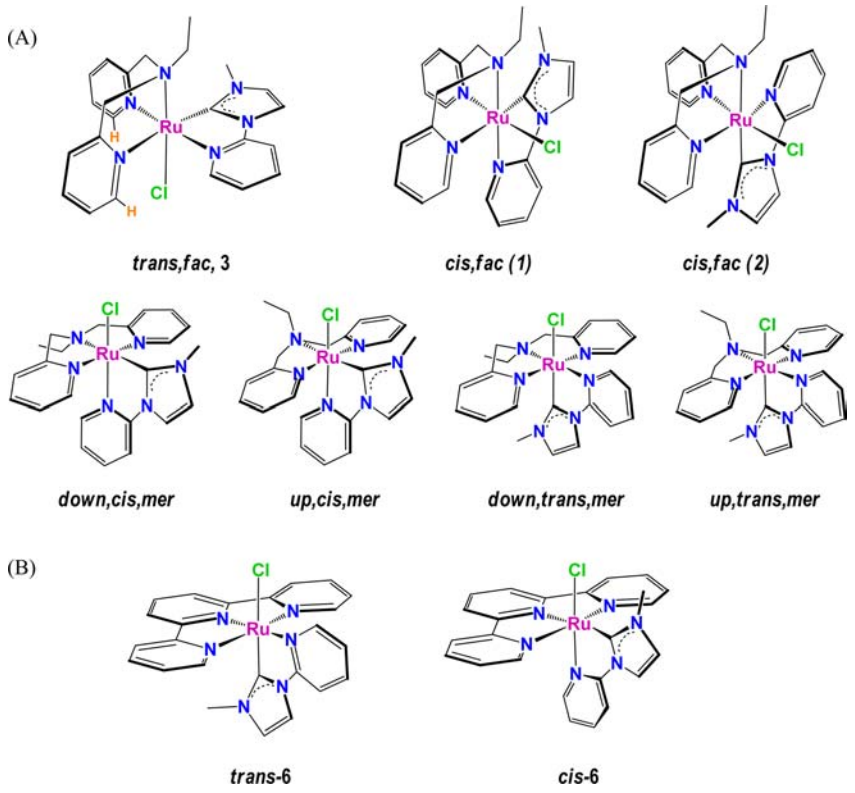

[a]The notation *fac* and *mer* refers to the facial or meridional disposition of the bpea ligand whereas *up* and *down* indicates the relative orientation of the ethyl group of bpea upon coordination. The H atoms involved in H-bonding in the *trans,fac* isomer are highlighted in orange.

the *trans* isomer, and thus, electronic factors, related to the strong σ-donor capacity of carbene NHC rings, must be appealed. Kinetic reasons such as distinctive *trans* effect during the coordination step can be the origin of the unequal ratio of isomers obtained, but the thermodynamics (spectroscopic and electrochemical properties) of the complexes also manifest the particular influence of the carbene ligand on the metal center as is described below.

The corresponding Ru−OH_2 complexes *trans,fac*-**5**, *trans*-**7**, and *cis*-**7** are easily obtained from the corresponding Ru−Cl complexes in the presence of Ag^+ in water. The geometry of the precursor chloro complex is kept in all cases except for the synthesis of *cis*-**7**, where a certain amount (up to 20%) of the corresponding *trans* isomer has been detected despite performing the reaction at dark. The isomerization upon substitution of the chloro ligand can be explained on the basis of the occurrence of a dissociative mechanism leading to a pentacoordinate intermediate species,[14] which would allow the aquo ligand to approach and bond the metal center through any side of the trpy ligand thus leading to either of the two isomers (see Supporting Information for a schematic representation of this process). However, it is striking that the mixture of isomeric Ru−OH_2 complexes is found only when starting from the *cis* chloro complex, manifesting again the major thermodynamic preference for the *trans* isomer in the complexes containing trpy and the CN-Me ligand. Once more, a different behavior is detected for the analogous complexes mentioned above that contain the pypz-Me ligand,[13] where only the *cis* aquo complex is obtained from the corresponding *cis* Ru−Cl.

At this level, we emphasize that both chloro complexes *trans*-**6** and *cis*-**6** are stable to light irradiation in solution. However, irradiation of the aquo complexes *trans*-**7** and *cis*-**7** with visible light in aqueous solution leads in any case to a partial isomerization reaching a steady state with a *cis*:*trans* ratio of roughly 35:65 independently of the starting isomer as shown by ^{1}H NMR experiments (see Supporting Information). Again, the analogous aquo complexes with pypz-Me behave in a different way leading in any case to a 50:50 isomeric mixture.

The structures of complexes *trans,fac*-**3**, *trans,fac*-**4**, and *cis*-**6** have been solved by X-ray diffraction analysis. The main crystallographic data for *trans,fac*-**3** and *cis*-**6** are summarized in Table 1 whereas their corresponding Ortep plots are gathered in Figure 1 (additional crystallographic information such as selected bond distances and angles for both complexes and the Ortep plot for the structure of *trans,fac*-**4** can be found in the Supporting Information). In both cases, the Ru metal centers adopt a distorted octahedral coordination with a disposition of the ligands according to the type of isomer obtained, as discussed above. For *trans,fac*-**3**, two enantiomeric forms are found within the crystal lattice, as expected from the asymmetry and the spatial arrangement of the CN-Me ligand. Most of the bond distances and angles are within the range of those usually found for this type of complex,[15,16] though the relatively long Ru−Cl bond distance found for both complexes which is around 2.44 Å is remarkable. This bond distance was considerably longer (2.47 Å) in the previously reported *trans*-**6** complex,[8] thus manifesting the remarkable *trans* influence exerted by the imidazolic NHC carbene ring.

The molecular units in complex *trans,fac*-**3** are organized in linear arrangements in the direction of the crystallographic *b*

dx.doi.org/10.1021/ic302863h | *Inorg. Chem.* 2013, 52, 5077−5087

Table 1. Crystal Data for Compounds *trans,fac*-3 and *cis*-6

	trans,fac-**3**	*cis*-**6**
empirical formula	$C_{23}H_{26}ClN_6F_6PRu$	$C_{28}H_{30}ClF_6N_6OPRu$
fw	667.99	748.07
cryst syst	orthorhombic	orthorhombic
space group	$Pna2_1$	*Pbca*
a [Å]	16.498(5)	13.41(2)
b [Å]	8.417(3)	15.63(3)
c [Å]	19.454(6)	28.17(5)
α [deg]	90	90
β [deg]	90	90
γ [deg]	90	90
V [Å^3]	2701.3(15)	5908(19)
formula units/cell	4	8
T, K	300(2)	100(2)
ρ_{calcd} [Mg/m^{-3}]	1.642	1.682
μ [mm^{-1}]	0.805	0.749
final *R* indices [$I > 2\sigma(I)$]	R1 = 0.0477[a]	R1 = 0.0893
	wR2 = 0.1178	wR2 = 0.1987
R indices [all data]	R1 = 0.0777	R1 = 0.1397
	wR2 = 0.1312	wR2 = 0.2259

[a] $R1 = \sum||F_o| - |F_o||/\sum|F_o|$. $wR2 = [\sum\{w(F_o^2 - F_c^2)^2\}/\sum\{w(F_o^2)^2\}]^{1/2}$, where $w = 1/[\sigma 2(F_o^2) + (0.0042P)^2]$ and $P = (F_o^2 + 2F_c^2)$.

axis, with the PF_6^- counterions allocated in the channels between the linear arrangements of the cationic complex (see Supporting Information). A similar arrangement is found for complex *cis*-**6**, in this case following the direction of the *a* crystal axis. Counterions are in all cases linked to complex cations through H-bonding with different H atoms of the ligands.

Spectroscopic Properties. All the complexes have been thoroughly characterized by 1D and 2D NMR techniques. The assignment of all the resonances is detailed in the Experimental Section, and the spectra registered are gathered in the Supporting Information. All the resonances found for complexes **3**−**7** are consistent with the structures obtained in the solid state. For the set of complexes with trpy ligand, the chemical shift of protons that are close to the monodentate ligand (Cl or H_2O) is clearly indicative of the isomer obtained in each case (for instance, the singlet assigned to the methyl protons H24 is found at 4.63 ppm in *cis*-**6** and at 2.90 in *trans*-**6**, due to the inductive effect of the Cl ligand in the close proximity of the methyl group; similarly, the pyridine H16 resonance is observed at 10.15 and 8.10 for *trans*-**6** and *cis*-**6**, respectively).

The UV−vis spectra of complexes *cis*-**6**, *cis*-**7**, *trans,fac*-**3**, *trans,fac*-**4**, and *trans,fac*-**5** display broad bands corresponding to dπ−π* MLCT and intraligand π−π* absorptions typical of Ru polypyridyl complexes.[17] The spectra registered in dichloromethane for the chloro and aquo complexes can be found in the Supporting Information (the bromo complex **4** displays a spectrum, not shown, almost identical to the one registered for the analogous *trans,fac*-**3** chloro complex). Table 2 collects the main absorption wavelengths and extinction coefficients together with a tentative assignment on the basis of the λ value and extinction coefficients.

Complexes *cis*-**6** and *cis*-**7** display a typical set of absorptions of MLCT dπ−π* and intraligand π−π* type, practically identical to those exhibited by their *trans* counterparts (entries 3 and 4), and also quite similar to the spectra of the analogous

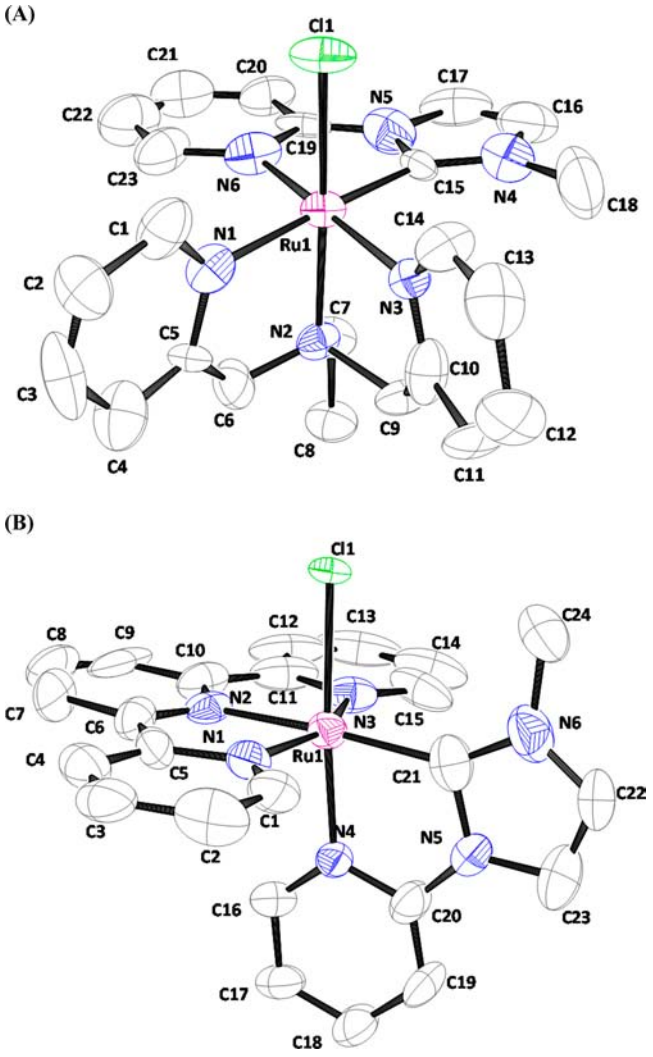

Figure 1. Ortep plots (ellipsoids at 50% probability level) and labeling schemes for the X-ray structure of compounds *trans,fac*-**3** (A) and *cis*-**6** (B).

$[RuX(trpy)(bpy)]^{n+}$complexes[17c] (X = Cl or H_2O, bpy = 2,2′-bipyridine), thus evidencing that the change of the bipyridine ligand by the carbene CN-Me does not have a significant influence on the electronic spectra in these compounds. On the other hand, in the case of complexes *trans,fac*-**3** and **5**, we observe only bands of type dπ−π*. The intraligand π−π* absorptions for complexes containing bpea are expected to appear at higher energies than those of complexes containing trpy (**6** and **7**) due to the lower aromatic character of the bpea ligand when compared to trpy, but in the case of complexes *trans,fac*-**3** and **5** the CN-Me ligand has also a remarkable effect in lowering the maximum wavelengths of the absorptions detected. This is clearly manifested when comparing the absorptions of complex *trans,fac*-**5** with those of the analogous complex containing bpy instead of CN-Me (entry 7),[20] and the overall effect is that, for complexes *trans,fac*-**3**/**5**, the dπ−π* MLCT bands are blue-shifted and the π−π* bands appear out of the range of λ allowed by the solvent.

On the other hand, the comparison of the MLCT bands for Ru−Cl and Ru−H_2O analogous complexes (entry 1 vs 2, or 5 vs 6) reveals a hypsochromic shift due to the replacement of the anionic Cl^- ligand by the neutral H_2O, given the strong σ- and π-donor ability of Cl^- which reduces the energy difference

dx.doi.org/10.1021/ic302863h | *Inorg. Chem.* 2013, 52, 5077−5087

Table 2. Main UV−Vis Spectroscopic Absorptions in CH_2Cl_2 for the Complexes Described

entry	compd	assignment	λ_{max}, nm (ε, M^{-1} cm^{-1})
1	*cis*-**6**	$\pi \rightarrow \pi^*$	268 (19 824), 280 (sh 14742), 320 (19 331)
		$d\pi \rightarrow \pi^*$	381 (5217), 498 (3898)
2	*cis*-**7**	$\pi \rightarrow \pi^*$	271 (17 275), 314 (21 462)
		$d\pi \rightarrow \pi^*$	364 (4996), 464 (4104)
3	*trans*-**6**[8]	$\pi \rightarrow \pi^*$	267 (16 636), 279 (sh 12 768), 316 (17 314)
		$d\pi \rightarrow \pi^*$	372 (5341), 490 (4316)
4	*trans*-**7**[8]	$\pi \rightarrow \pi^*$	272 (18 306), 315 (21 670)
		$d\pi \rightarrow \pi^*$	362 (5250), 463 (4494)
5	*trans,fac*-**3**	$d\pi \rightarrow \pi^*$	245 (sh 7326), 270 (3803), 380 (4971), 399 (4584)
6	*trans,fac*-**5**	$d\pi \rightarrow \pi^*$	272 (5929), 301 (3432), 358 (5067), 382 (4639)
7	*trans,fac*-[Ru(bpea)(bpy)(H_2O)]$^{2+}$,[20]	$\pi \rightarrow \pi^*$	246 (18 755), 292 (31 420)
		$d\pi \rightarrow \pi^*$	360 (12 257), 468 (6048)

between full d orbitals of the metal and empty π^* orbitals of the ligands.

The pK_a of the Ru-aqua complexes *trans,fac*-**5** and *cis*-**7** has been evaluated through spectrophotometric acid−base titrations in aqueous solution[18] (see Supporting Information). Upon addition of base, a red-shift of the maximum wavelength is detected for the MLCT bands that can be explained by the increase of the electron density coming from the anionic hydroxyl ligand, which destabilizes the d orbitals of the metal thus lowering the transition energy in a similar way to that described above for chloride ligand.[19] A set of isosbestic points is found in each case (237, 251, 277, 389, and 527 nm for *trans,fac*-**5**; 261, 331, 416, and 480 nm for *cis*-**7**), indicative of a net $Ru^{II}-OH_2 \leftrightarrows Ru^{II}-OH$ transformation. The pK_a value determined for *cis*-**7** was 10.91. However, in the case of *trans,fac*-**5** the complete conversion to $Ru^{II}-OH$ could not be achieved even at pH values above 12, and consequently, the exact pK_a value cannot be calculated. The lower acidity of *trans,fac*-**5** when compared to *cis*-**7** is in agreement with the higher electron-donor capacity of the bpea ligand with regard to trpy (which renders the metal center much less acidic)[20] together with the fact that, in complex *trans,fac*-**5**, the aqua ligand is placed *trans* to the aliphatic N atom of bpea thus facilitating the transmission of the electron density.

Redox Properties. The redox properties of the compounds have been determined by cyclic voltammetry (CV) and spectrophotometric titration experiments in the case of aquo complexes. The chloro complexes *trans,fac*-**3** and *cis*-**6** present a reversible, monoelectronic Ru(III/II) wave at 0.66 and 0.77 V versus SSCE, respectively (see Supporting Information), with a 0.11 V difference that can be attributed to the major electron-withdrawing character of trpy ligand with regard to bpea. However, it is interesting to compare these $E_{1/2}$ values with the one displayed by the isomeric *trans*-[RuCl(CN-Me)(trpy)]$^+$ (*trans*-**6**) complex,[8] which is of 0.88 V despite containing identical ligands as *cis*-**6**. This difference reveals a particular behavior in complexes containing carbene ligands such as CN-Me, where the relative position of the ligands around the metal also determines the electrochemical properties of the complex (the analogous *cis*/*trans* isomers of chloro complexes containing trpy and pypz-Me[13] display almost identical $E_{1/2}$ values). In the specific case of *trans*-**6**, the remarkably high $E_{1/2}$ Ru(III/II) value probably arises from the large Ru−Cl bond distance of 2.47 Å provoked by the presence of the carbene ring in *trans* to Cl.

The redox properties of Ru-aqua complexes are pH dependent due to the capacity of the aqua ligand to lose protons upon oxidation of the complex as indicated in eq 1,[21] which also makes the upper oxidation states easily accessible:

$$L_5Ru^{II}-OH_2 \underset{+1H^+,+1e^-}{\overset{-1H^+,-1e^-}{\rightleftharpoons}} L_5Ru^{III}-OH \underset{+1H^+,+1e^-}{\overset{-1H^+,-1e^-}{\rightleftharpoons}} L_5Ru^{IV}=O \quad (1)$$

The reversibility of these redox processes constitutes the basis for the use of this kind of complex in redox catalysis. In most cases, the two monoelectronic redox processes indicated in eq 1, corresponding to the Ru(III/II) and Ru(IV/III) redox couples, can be observed in cyclic voltammetry. However, some Ru complexes have been described in the literature where the two redox processes occur simultaneously:[7−9,13]

$$L_5Ru^{II}-OH_2 \underset{+2H^+,+2e^-}{\overset{-2H^+,-2e^-}{\rightleftharpoons}} L_5Ru^{IV}=O \quad (2)$$

The complete thermodynamic information regarding the Ru-aqua type of complex can be extracted from the Pourbaix diagrams, displayed in Figure 2 for complexes *trans,fac*-**5** and

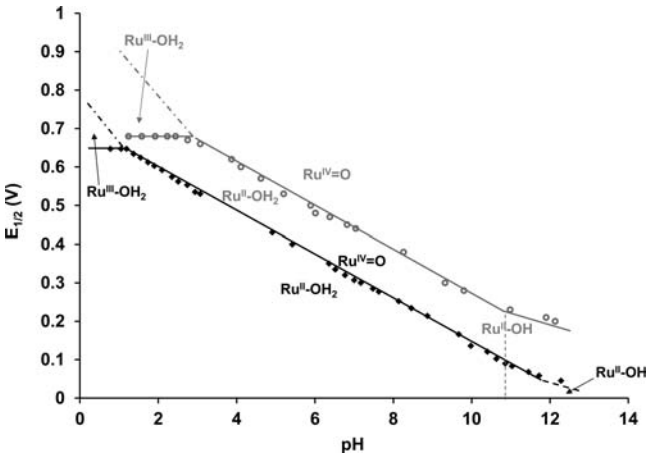

Figure 2. Pourbaix diagram for the aquo complexes *trans,fac*-**5** (black pattern) and *cis*-**7** (gray pattern). The main proton compositions are indicated.

cis-**7**. As can be observed, a unique pH-dependent redox process is found through a wide pH range (at pH values higher than 2.7 for *cis*-**7** and above 1.2 for *trans,fac*-**5**). The dependence of $E_{1/2}$ versus pH is linear with a slope of approximately −59 mV per pH unit, indicative of the transfer of an equivalent number of protons and electrons as stated in eq 2. The change of slope to a roughly −30 mV value at a pH

dx.doi.org/10.1021/ic302863h | *Inorg. Chem.* 2013, 52, 5077−5087

value of around 10.8 for *cis*-**7** is indicative of deprotonation of the $Ru^{II}-OH_2$ (pK_a(II) value) leading to a basic pH range where the bielectronic redox process is accompanied by the exchange of only one proton. The pK_a(II) value inferred from the Pourbaix diagram is consistent with the one obtained from acid–base spectrophotometric titration (10.91). For *trans,fac*-**5**, an estimated pK_a value could be suggested at a value around 12, which is in accordance with the fact that complete deprotonation could not be attained in acid–base titration as stated above. Finally, the horizontal lines at acidic pH indicate the transfer of only one electron that occurs between the $Ru^{II}-OH_2$ and the $Ru^{III}-OH_2$ forms (without proton exchange). The end of this area, at pH values of 1.2 and 2.7 for *trans,fac*-**5** and *cis*-**7**, respectively, corresponds in each case to the pK_a of the oxidized $Ru^{III}-OH_2$ form (pK_a(III)).

To confirm the occurrence of bielectronic waves we have performed a redox spectrophotometric titration of *trans,fac*-**5** and *cis*-**7** with Ce(IV) as oxidant, and the sets of spectra obtained are shown in Figure 3 and in the Supporting

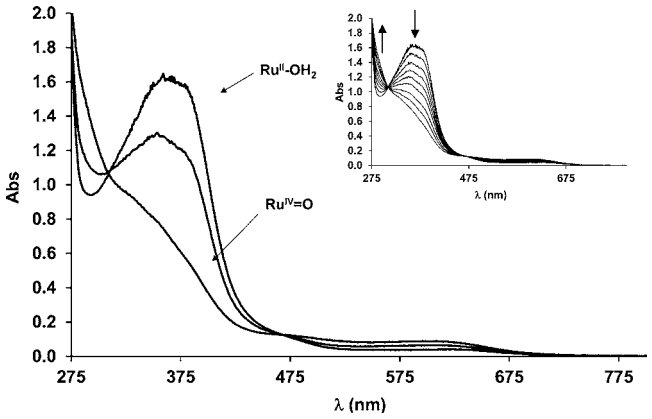

Figure 3. Redox spectrophotometric titration performed by sequential addition of 50 μL of 10^{-2} M of Ce(IV) (up to 2 equiv) to 25 mL of a 10^{-4} M solution of *trans,fac*-**5** in 0.1 M HCl.

Information, respectively. In both cases, the evolution of the spectra along the addition of 2 equiv of Ce(IV) leads to a featureless UV–vis spectrum characteristic of $Ru^{IV}=O$ species[17c,22] with the occurrence of isosbestic points throughout the whole titration (254, 308, and 467 nm for *trans,fac*-**5**; 295, 344, and 612 nm for *cis*-**7**), thus indicating a direct, 2-electron transformation from Ru(II) to Ru(IV).

Table 3 summarizes the electrochemical data and the pK_a of the aquo complexes described together with those of analogous complexes for comparison purposes. In all cases, the *cis* or *trans* configuration (relative to the aquo ligand) is determined by considering the ligand with higher σ-donor capacity than that of the pyridyl ring. Taking as reference the well-known $[Ru(trpy)(bpy)(H_2O)]^{2+}$ complex (entry 1), one can see that the replacement of bpy by an anionic ligand such as picolinate (entries 7 and 8) considerably lowers both the Ru(III/II) and Ru(IV/III) $E_{1/2}$ values as expected from the higher σ-donor ability of the anionic ligand. It is interesting to note that a similar effect is attained by replacing trpy by the more σ-donor (and less π-acceptor) bpea ligand (entry 9), though both are neutral ligands. On the other hand, the replacement of bpy in $[Ru(trpy)(bpy)(H_2O)]^{2+}$ by the anionic pyrpy-O ligand (pyrpy-O corresponds to 3-hydroxy-2,4-dimethyl-5-(2-pyridyl)-pyrrolate, entry 2) produces a dramatic change in the redox properties, leading to the occurrence of a bielectronic Ru(IV/II) process. The $E_{1/2}$(IV/II) value observed is virtually the same as those for other complexes with the same *trans* geometry but having one or three carbene rings in the complex structure (entries 3 and 5, respectively). However, the analogous complexes with *cis* geometry (entries 4 and 6) present also a bielectronic process but at a potential value around 0.12–0.13 V lower than their *trans* counterparts. Thus, for the bielectronic complexes, we note that the coordination of the σ-donor ligand in *trans* increases the $E_{1/2}$(IV/II) redox potential when compared to the corresponding *cis* isomer, while in the case of monoelectronic complexes this behavior is reversed (entries 7 and 8). Finally, the replacement of trpy in the monocarbene complexes *trans*- or *cis*-**7** by bpea (entry 10) produces a significant decrease of the Ru(IV/II) $E_{1/2}$ value still keeping the bielectronic process, converting complex *trans,fac*-**5** into the one exhibiting the lowest potential value among the series of bielectronic compounds although it contains only one carbene ring.

Regarding the pK_a(II) values gathered in Table 3, we can observe that complexes containing carbene and/or bpea ligands (entries 3–6, 9, and 10) present higher values (above 10.9) than the rest of complexes (pK_a(II) of 9.7–10, entries 1, 2, 7, and 8), with independence of the type of ligands (neutral or anionic) that they contain or whether they exhibit a bielectronic

Table 3. pK_a and Electrochemical Data (pH = 7, $E_{1/2}$ in V vs SSCE) for the Aquo Complexes Described in This Work and Others Previously Reported

entry	complex[a] (T)(D)Ru–OH_2	$E_{1/2}$(III/II)	$E_{1/2}$(IV/III)	$E_{1/2}$(IV/II)	ΔE^b	pK_a(II)	pK_a(III)	ref
1	(trpy)(bpy)Ru–OH_2	0.49	0.62		0.13	9.7	1.7	21a
2	*trans*-(trpy)(pyrpy-O)Ru–OH_2			0.55	≤0	9.7	1.21	13
3	*trans*-**7**			0.57	≤0	11.00	3.08	8
4	*cis*-**7**			0.44	≤0	10.91	2.7	this work
5	*trans*-(CNC)(CN-Bu)Ru–OH_2			0.56	≤0	11.9	4.8	7
6	*cis*-(CNC)(CN-Bu)Ru–OH_2			0.44	≤0	12.3	3.0	7
7	*trans*-(trpy)(pic)Ru–OH_2	0.21	0.45		0.24	10.0	2	22c
8	*cis*-(trpy)(pic)Ru–OH_2	0.38	0.56		0.18	10.0	3.7	22c
9	(bpea)(bpy)Ru–OH_2	0.34	0.46		0.12	11.1	1.2	20
10	*trans,fac*-**5**			0.32	≤0	~12	1.19	this work

[a]Abbreviation of tridentate ligand T: CNC = 2,6-bis(butylimidazol-2-ilidene)pyridine. Abbreviation of didentate ligand D: pic =2-picolinate; bpy = 2,2′-bipyridine; CN-Bu = *N*-butyl-*N*′-2-pyridylimidazolium; pyrpy-O = 3,5-dimethyl-4-hydroxo-2-(2-pyridyl)pyrrolate. [b]$\Delta E = E_{1/2}$(IV/III) – $E_{1/2}$(III/II) (in V).

dx.doi.org/10.1021/ic302863h | *Inorg. Chem.* 2013, 52, 5077–5087

or two monoelectronic processes. For the case of pK_a(III), the higher values are exhibited by the carbene complexes (with the exception of *trans,fac*-**5**, entry 10), although there is not a clear trend since the picolinate complexes (entries 7 and 8) also present relatively low acidic $Ru^{III}-OH_2$ forms.

A previous report of Meyer et al.[23] establishes an empirical correlation between $\Delta E_{1/2}$ (defined as the difference between the IV/III and III/II redox couples for the $Ru-OH_2$ type of complexes, Table 3) vs ΣE_L, which is the sum of a series of parameters calculated by Lever[23a] for the nonaqua ligands attached to the Ru metal center. The Meyer–Lever correlation, displayed in Figure 4, shows that the family of $Ru-OH_2$

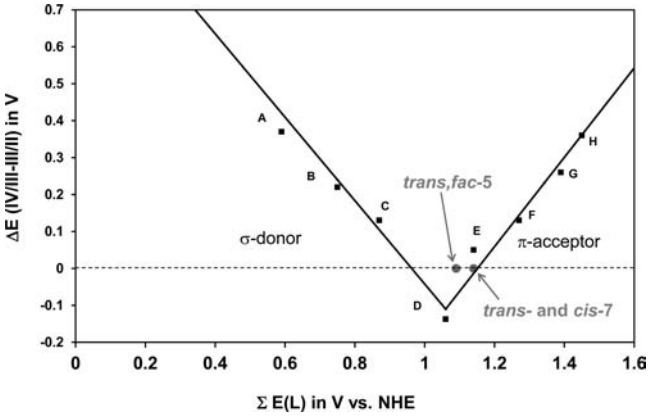

Figure 4. Meyer–Lever plot of observed $\Delta E_{1/2}$ vs $\sum E_L$. Molecular formulas for the complexes represented: (A) $[Ru(trpy)(acac)(OH_2)]^+$ (acac is acetylacetonate); (B) *cis*-$[Ru(trpy)(pic)(OH_2)]^+$ (pic is picolinate); (C) $[Ru(trpy)(tmen)(OH_2)]^{2+}$ (tmen is *N,N,N,N*-tetramethylethylenediamine); (D) *cis*-$[Ru(CNC)(CN\text{-}Bu)(OH_2)]^{2+}$ (CNC is 2,6-bis(butylimidazol-2-ilidene)pyridine; CN-Bu is *N*-butyl-*N*′-2-pyridylimidazolium); (E) -$[Ru(CNC)(bpy)(OH_2)]^{2+}$ (bpy is 2,2′-bipyridine); (F) $[Ru(trpy)(bpy)(OH_2)]^{2+}$; (G) $[Ru(bpy)_2(OH_2)(PPh_3)]^{2+}$; (H) $[Ru(trpy)(dppene)(OH_2)]^{2+}$ (dppene is *cis*-1,2-bis(diphenylphosphino)ethylene).

complexes lay into two different lines depending on the σ-donating or π-accepting character of the ligands attached to the Ru metal center, and that the right ligand combination, in order to reach the $\Delta E \leq 0$ zone (which involves the spontaneous disproportion of the Ru(III) oxidation state, i.e. a bielectronic redox process), should have an ΣE_L value between approximately 0.95 and 1.2. The ΣE_L parameters for *trans,fac*-**5** and *cis*-**7** have been determined to be of 1.09 and 1.14, respectively, nicely placing both aquo complexes into the $\Delta E \leq 0$ area of the Meyer–Lever plot as has been determined experimentally (see Supporting Information for details of the calculation). A recent report based on DFT calculations[24] states that a correlation can be established between the number of carbene units present in a Ru complex and the Ru(III/II) and Ru(IV/III) redox couples in such a way that the higher the number of carbene units, the higher the $E_{1/2}$(III/II) value and the lower the $E_{1/2}$(IV/III). As the number of carbene units increases, the point where ΔE is equal or below zero can be more easily attained. In our case, however, a unique carbene ring has been shown to be enough to reach the Ru(III) disproportion in the two complexes described.

Catalytic Epoxydation. To study the catalytic properties and the geometric and electronic effects of tridentate (meridional/facial) and didentate (*cis*/*trans*) ligands of complexes *trans,fac*-**5** and *cis*-**7**, we have applied the same conditions used for the evaluation of the catalytic activity of *trans*-**7**.[8] Table 4 summarizes the results obtained with both catalysts and also includes the results obtained with *trans*-**7** for comparison purposes. Blank experiments performed in absence of catalyst did not yield any oxidation product.

Steric and electronic factors of both the complexes and the substrates should be considered to rationalize the differences in performance observed in some cases. For styrene substrate (entry 1), a comparison between the performances of the three complexes provides evidence of a reactivity governed exclusively by electronic factors with a conversion degree increasing in parallel to the redox Ru(IV/II) potential of the catalysts (*trans*-**7** > *cis*-**7** > *trans,fac*-**5**). However, the selectivity is better for *trans,fac*-**5** that presents the lowest redox potential. According to the literature, the epoxide selectivity is affected by steric effects[25] but also by the acidity of catalysts,[26] which lead to a rearrangement of the epoxide thus producing a decrease in selectivity. In the case of styrene, the improvement in selectivity is in agreement with the increasing pK_a(II) value in the order *cis*-**7** < *trans*-**7** < *trans,fac*-**5**. (see Table 3).

On the other hand, focusing the attention in the initial conversion rates v_i, one can observe that complex *trans,fac*-**5** presents considerably higher rates for almost all the substrates studied, whereas *cis*-**7** is the slowest catalyst as average. This fact is in agreement with the higher σ-donor and lower π-acceptor capacity of the bpea ligand in comparison to trpy, which could lead to a more nucleophilic active Ru=O species, but structural factors can also have an influence. Indeed, the structural arrangement of the ligands in the three catalysts seems to be more favorable for *trans*-**7** and *trans,fac*-**5**, where only C–H pyridyl atoms are located in the surroundings of the Ru=O

Table 4. Catalytic Epoxidation of Different Alkenes with *trans,fac*-5, *trans*-7, and *cis*-7 Using $PhI(OAc)_2$ as Oxidant[a]

		trans,fac-**5**		*trans*-**7**			*cis*-**7**			
entry	complex alkene	conv	sel[b]	v_i	conv	sel	v_i	conv	sel	v_i
1	styrene	48	93.4		>99	61		60	50	
2	*trans*-stilbene	>99[c]	99	250	90	89	13.6	90	66	7.7
3	*cis*-*β*-methylstyrene	85	94	38.5	81	94	6.1	>99	92	9.9
4	cyclooctene	>99	99.5	25.4	>99	94	8.4	85	98	5.5
5	1-octene	96	99.6	13.9	98	80	8.6	15 (70)[d]	98 (96)[d]	1.2
6	4-vinylcyclohexene	80.5	97.2	7.8	99	97	10.9	96.5	93	8.6

[a]Conditions: alkene (50 mM), complex (0.5 mM), oxidant $PhI(OAc)_2$ (100 mM), CH_2Cl_2 (2.5 mL), 25 °C, 24 h, biphenyl (15 mM) as internal standard. Conversion (conv) and selectivity (sel) values are given in %, and initial reaction rates v_i in 10^{-6} mol h^{-1} [b]Selectivity for epoxide, [yield/conversion] × 100. Byproducts have been determined in most cases to be the corresponding ketones or aldehydes. [c]Analysis performed after 3 h. [d]In parentheses, analysis performed after 48 h.

dx.doi.org/10.1021/ic302863h | *Inorg. Chem.* 2013, 52, 5077–5087

group, in contrast with *cis*-**7**, which presents a methyl group that can convey steric hindrance (then producing a decrease in the reaction rates for this catalyst, as is observed in most substrates). Moreover, *trans,fac*-**5** presents the pyridyl rings of bpea in a perpendicular fashion with respect to the equatorial plane of the complex, and this arrangement could favor the approach of aromatic substrates through π-interactions[27] (see Supporting Information for a schematic representation of this effect). Indeed, the two aromatic substrates (*trans*-stilbene and *cis*-β-methylstyrene, entries 2 and 3) are epoxidized by *trans,fac*-**5** with the highest v_i values. It is particularly noticeable in the case of *trans*-stilbene, which is completely epoxidized within 3 h reaction with excellent selectivity. Finally, in *trans,fac*-**5** the atom in *trans* position with regard to the Ru=O active site is the aliphatic N atom of bpea that can in principle generate a more nucleophilic oxo group[28] thanks to the more effective transmission of the electron density, which would also be in agreement with the higher rates displayed by this complex especially for activated substrates. A similar argument (besides the steric hindrance mentioned above) could explain the slightly better performance of complex *trans*-**7** with regard to *cis*-**7**, since in *trans*-**7** the Ru=O group is in *trans* with regard to the more σ-donor carbene ring whereas in *cis*-**7** this position is occupied by a pyridyl ring. The low reaction rates displayed by *cis*-**7** are in some cases accompanied by a decrease in the selectivity for the epoxide (entries 1 and 2).

Finally, it is worth mentioning here that the epoxidation of *cis*-β-methylstyrene (entry 3) is stereospecific for the *cis* epoxide with all the catalysts. This is in agreement with the occurrence of bielectronic redox processes on the catalysts, which can lead to a concerted mechanism of O atom transfer from the Ru=O active group.[4,29] Catalysts that operate by a radical mechanism as Mn-salen complexes[30] and some other ruthenium oxo complexes[5b] have been described to generate a mixture of *cis*/*trans* epoxides. The design of bielectronic catalysts is thus of great importance to achieve good selectivity degrees. The epoxidation of 4-vinylcyclohexene (entry 6) is also regiospecific, with the epoxidation taking place exclusively at the cyclohexene ring.

In conclusion, we have carried out the synthesis and characterization of new examples of the scarce Ru(II)−OH_2 complexes displaying bielectronic processes, where the presence of carbene NHC ligands seems to be relevant for the attainment of a Ru(IV/II) redox couple but with independence of the *cis* or *trans* geometry. The comparison of complexes bearing the meridional trpy or the facial bpea ligand provide evidence that both electronic and steric factors seem to be more favorable for the bpea ligand as epoxidation catalyst, revealing higher reaction rates and selectivities for the *trans,fac*-**5** complex. The occurrence of a σ-donor ligand in *trans* fashion with regard to the aqua/oxo ligand also favors the catalytic performance.

EXPERIMENTAL SECTION

Materials. All reagents used in the present work were obtained from Aldrich Chemical Co. and were used without further purification. Reagent grade organic solvents were obtained from SDS, and high purity deionized water was obtained by passing distilled water through a nanopure Mili-Q water purification system. $RuCl_3 \cdot 2H_2O$ was supplied by Johnson and Matthey Ltd. and was used as received.

Preparations. Ligands CN-Me (*N*-methyl-*N*′-2-pyridylimidazolium bromide)[31] and bpea (*N*,*N*-bis(2-pyridylmethyl)ethylamine)),[32] and the complexes $[Ru^{II}Cl_2(bpea)dmso]$, **1**,[10] $[Ru^{III}Cl_3(trpy)]$, **2**,[11] *trans*-$[RuCl(CN\text{-}Me)(trpy)]PF_6$, *trans*-**6**,[8] and *trans*-$[Ru(CN\text{-}Me)(trpy)(H_2O)](PF_6)_2$, *trans*-**7**,[8] were prepared as described in the literature. All synthetic manipulations were routinely performed under nitrogen atmosphere using Schlenk tubes and vacuum line techniques.

***trans,fac*-$[Ru^{II}Cl(CN\text{-}Me)(bpea)](PF_6)$ and *trans,fac*-$[Ru^{II}Br(CN\text{-}Me)(bpea)](PF_6)$, *trans,fac*-3·0.5$CH_2Cl_2$ and *trans,fac*-4·2.5CH_2Cl_2.** *Method 1.* A sample of **1** (100 mg, 0.209 mmol) was dissolved in 20 mL of diethyleneglycol, and it was stirred at room temperature for 30 min under N_2 atmosphere. After that the mixture was heated to 60 °C, and then, 50.18 mg (0.209 mmol) of [HCN-Me]Br dissolved in 2 mL of diethyleneglycol and 0.09 mL (0.627 mmol) of NEt_3 were added. The reaction mixture was heated at 150 °C for 3 h. After this time, it was cooled to room temperature, and then, 1 mL of a saturated aqueous NH_4PF_6 solution and 20 mL of water were subsequently added. A yellow precipitate of $[Ru^{II}X(CN\text{-}Me)(bpea)](PF_6)$ (X = Cl^- or Br^-) appeared which was filtered, washed with water and ether, and dried under vacuum. In order to separate the chloro complex from the bromo complex, the resulting precipitate was purified over silica column using dichloromethane/acetone (9/1) as eluent. The first orange fraction corresponds to $[Ru^{II}Br(CN\text{-}Me)(bpea)](PF_6)$, *trans,fac*-**4**, and the second yellow fraction corresponds to $[Ru^{II}Cl(CN\text{-}Me)(bpea)](PF_6)$, *trans,fac*-**3**. The solutions of both complexes were evaporated to dryness, and the resulting solid was recrystallized from a mixture of dichloromethane and pentane (1:1, v/v), washed with ether and then pentane, and dried under vacuum. Yield of *trans,fac*-**3**: 48 mg (34.4%). Yield of *trans,fac*-**4**: 20 mg (13.4%).

Method 2. In order to synthesize only the *trans,fac*-**3** complex, it was prepared in a manner identical to the previous method except that the reaction was performed in the presence of an excess of LiCl (12 equiv per Ru). The yellow solid obtained after the addition of 1 mL of a saturated aqueous NH_4PF_6 solution corresponds to complex *trans,fac*-**3**. Yield: 57%. Anal. Found (Calcd) for $C_{23}H_{26}N_6ClRuPF_6 \cdot 0.5CH_2Cl_2$: C, 39.51 (39.73); N, 11.85 (11.82); H, 4.10 (3.83). ^{1}H NMR (600 MHz, acetone-d_6, 25 °C) δ (ppm): 9.61 (ddd, J = 5.4, 1.6, 0.8 Hz, H1), 9.49 (ddd, J = 5.4, 1.6, 0.8 Hz, H14), 8.34 (d, J = 2.3 Hz, H17), 8.25 (ddd, J = 5.7, 1.6, 0.7 Hz, H23), 8.06 (dt, J = 8.3, 0.9 Hz, H20), 7.94 (td, J = 8.3, 7.4, 1.6 Hz, H21), 7.89 (td, J = 7.7, 1.6 Hz, H3), 7.70 (td, J = 7.7, 1.6 Hz, H12), 7.54 (d, J = 7.8 Hz, H4), 7.49 (td, J = 7.8, 1.2 Hz, H2), 7.46 (d, J = 2.3 Hz, H16), 7.40 (d, J = 7.6 Hz, H11), 7.26 (t, J = 5.8 Hz, H13), 7.20 (td, J = 5.9, 1.2 Hz, H22), 4.51 (d, J = 16.5 Hz, H9a), 4.37 (d, J = 16.4 Hz, H6a), 4.27 (t, J = 15.8 Hz, H9b), 4.25 (t, J = 15.8 Hz, H6b), 3.46 (s, H18, 3H), 2.55 (dd, J = 13.4, 7.2 Hz, H7b), 2.31 (dd, J = 13.4, 7.1 Hz, H7a), 0.99 (t, J = 7.2 Hz, H8, 3H). ^{13}C NMR (151 MHz, acetone-d_6, 25 °C) δ (ppm): 204.78 (C15), 162.82 (C10), 161.03 (C5), 156.21 (C19), 152.94 (C14), 152.76 (C23), 150.81 (C1), 137.84 (C21), 137.68 (C3), 136.00 (C12), 125.88 (C16), 124.83 (C2), 124.28 (C13), 122.56 (C4), 121.95 (C22), 121.72 (C11), 116.98 (C17), 111.33 (C20), 68.96 (C9), 67.13 (C6), 63.14 (C7), 36.19 (C18), 8.77 (C8). NOEs: H1 with H23, H23 with H6b, H4 with H6a, H17 with H20, and H11 with H9a. For the NMR assignment we have used the same numbering scheme as for the X-ray structure displayed in Figure 1. IR (ν_{max}, cm^{-1}): 2368 (s), 1610 (m),1490 (m), 1349 (m), 1255 (w), 836 (s) 769 (m), 555 (s). $E_{1/2}$(III/II) (CH_2Cl_2 + 0.1 M TBAH): 0.66 V vs SSCE. UV−vis (CH_2Cl_2): λ_{max}, nm (ε, M^{-1} cm^{-1}) 245 (7326), 270 (3803), 380 (4971), 399 (4584). ESI-MS (m/z): 523.1 $[M - PF_6]^+$.

Data for *trans,fac*-**4**·2.5CH_2Cl_2 follow. Anal. Found (Calcd) for $C_{23}H_{26}N_6BrRuPF_6 \cdot 2.5CH_2Cl_2$: C, 33.33 (33.12); N, 8.87 (9.08); H, 3.81 (3.38). ^{1}H NMR (200 MHz, acetone-d_6, 25 °C) δ (ppm): 9.77 (d, H1), 9.63 (d, H14), 8.34 (d, H18), 8.25 (d, H23), 8.06 (d, H20), 7.94 (d, H21), 7.89 (t, H3), 7.70 (t, H12), 7.54 (d, H4), 7.49 (t, H2), 7.46 (d, H17), 7.40 (d, H11), 7.26 (t, H13), 7.20 (t, H22), 4.51 (d, H9a), 4.37 (d, H6a), 4.27 (t, H9b), 4.25(t, H6b), 3.46 (s, H16, 3H), 2.55 (d, H7b), 2.31 (d, H7a), 0.99 (t, H8, 3H). For the NMR assignment we have used the same numbering scheme as for the X-ray structure displayed in Figure 1. $E_{1/2}$(III/II) (CH_2Cl_2 + 0.1 M TBAH): 0.67 V versus SSCE. UV−vis (CH_2Cl_2): λ_{max}, nm (ε, M^{-1} cm^{-1}) 269 (3295), 377 (4915). ESI-MS (m/z): 567.2 $[M - PF_6]^+$.

***trans,fac*-$[Ru^{II}(CN\text{-}Me)(bpea)OH_2](PF_6)_2$, *trans,fac*-5.** A 25 mg (0.037 mmol) sample of *trans,fac*-**3** and a 12.57 mg (0.074 mmol)

dx.doi.org/10.1021/ic302863h | *Inorg. Chem.* 2013, 52, 5077−5087

sample of $AgNO_3$ were placed in a round-bottom flask together with 15 mL of H_2O. The resulting mixture was refluxed for 3 h in darkness. After this time the reaction was cooled to room temperature (RT) and then in an ice bath, and the AgCl formed was removed by filtration through Celite. Afterward, a 1 mL sample of saturated aqueous solution of NH_4PF_6 was added to the filtrate, and the solvent was removed slowly in a rotary evaporator until precipitation of a green solid that was filtered, washed with ether and then pentane, and dried under vacuum. Yield: 20 mg (68%). Anal. Found (Calc) for $C_{23}H_{28}N_6ORuP_2F_{12}$: C, 34.75 (34.73); N, 10.01 (10.5); H, 3.87 (3.54). ^{1}H NMR (600 MHz, acetone-d_6/10% OD_2, 25 °C) δ (ppm): 9.01 (d, J = 5.1 Hz, H1), 8.81 (d, J = 5.1 Hz, H14), 8.42 (d, H17), 8.40 (d, J = 5.6 Hz, H23), 8.15 (d, J = 8.2 Hz, H20), 8.06 (t, J = 7.7 Hz, H21), 7.95 (t, J = 7.4 Hz, H3), 7.78 (t, J = 7.8 Hz, H12), 7.60 (d, J = 8.0 Hz, H4), 7.55 (t, J = 6.3 Hz, H2), 7.53 (s, H16), 7.46 (d, J = 8.0 Hz, H11), 7.35 (t, J = 5.9 Hz, H13), 7.31 (t, J = 6.0 Hz, H22), 4.48 (d, J = 17.0 Hz, H9a), 4.37 (d, J = 16.4 Hz, H6a), 4.22 (d, J = 16.7 Hz, 9Hb), 4.22 (d, J = 16.7 Hz, H6b), 3.55 (s, H18, 3H), 2.33 (m, H7b), 2.13 (m, H7a), 0.92 (t, J = 7.1 Hz, H8, 3H). ^{13}C NMR (151 MHz, acetone-d_6/10% D_2O, 25 °C) δ (ppm): 200.87 (C15), 162.41 (C10), 160.57 (C5), 156.31 (C19), 153.51 (C14), 150.34 (C23), 149.30 (C1), 139.69 (C21), 138.47 (C3), 136.99 (C12), 126.64 (C16), 125.35 (C2), 124.82 (C13), 123.14 (C4), 122.76 (C22), 122.23 (C11), 117.79 (C17), 112.02 (C20), 69.28 (C9), 67.92 (C6), 63.44 (C7), 36.40 (C18), 8.58 (C8). IR (ν_{max}, cm^{-1}): 3507 (w), 3200 (s), 2362 (m), 1625 (m), 1450 (m), 1340 (m), 1200 (m), 831 (s) 767 (s), 551 (s). $E_{1/2}$(IV/II), phosphate buffer pH = 7: 0.32 V versus SSCE. UV−vis phosphate buffer pH = 7: λ_{max}, nm (ε, M^{-1} cm^{-1}) 266 (13 787), 347 (10 847). CH_2Cl_2: 272 (5929), 301 (3432), 358 (5067), 382 (4639). ESI-MS (m/z): 505.1 $[M - H^+ - 2PF_6^-]^+$.

***cis*-[Ru^{II}Cl(CN-Me)(trpy)](PF$_6$), *cis*-6·0.45CH$_2$Cl$_2$.** A sample of **2** (100 mg, 0.218 mmol) and LiCl (18.48 mg, 0.436 mmol) were dissolved in a 3:1 EtOH/H_2O mixture (40 mL) under N_2 atmosphere. Then, NEt_3 (0.06 mL, 0.436 mmol) was added, and the brown mixture was stirred for 30 min at room temperature, upon which it progressively became a dark-green solution. At this point, the [HCN-Me]Br ligand (52.33 mg, 0.218 mmol) dissolved in 2 mL of degassed 3:1 EtOH/H_2O was added, and the resulting solution was refluxed overnight. Upon cooling to room temperature, the solution was filtered on a frit to eliminate small amounts of a black solid. Afterward, 2 mL of a saturated NH_4PF_6 aqueous solution was added to the solution, and the volume was reduced at low pressure until a precipitate appeared. The resulting solid was filtered on a frit, washed with water and ether, and dried in vacuum. The dark-brown solid obtained was purified by chromatography over alumina using dichloromethane as eluent and an increasing gradient of methanol (0−1%). A first violet fraction corresponding to *cis*-**6** and a second brown fraction corresponding to its *trans* isomer were obtained, together with an orange fraction corresponding to $[Ru(trpy)_2]^{2+}$ byproduct. After column chromatography, *cis*-**6** was recrystallized from a mixture of dichlomethane and ether (1:1, v/v). Anal. Found (Calcd) for $C_{24}H_{20}N_6ClRuPF_6$·0.45CH_2Cl_2: C, 41.54 (41.23); N, 11.40 (11.79); H, 3.01 (2.96). ^{1}H NMR (600 MHz, acetone-d_6, 25 °C) δ (ppm): 8.74 (d, J = 8.1 Hz, H7, H10), 8.57 (d, J = 8.0 Hz, H4, H13), 8.50 (d, J = 2.4 Hz, H24), 8.29 (t, J = 8.1 Hz, H9), 8.10 (d, J = 5.4 Hz, H1, H16), 7.99 (d, J = 8.3 Hz, H20), 7.92 (td, J = 7.8, 6.3 Hz, H3, H14), 7.83 (d, J = 2.3 Hz, H23), 7.75 (tq, J = 8.7, 7.4, 1.5 Hz, H19), 7.43 (dt, J = 5.8, 0.9 Hz, H17), 7.31 (tq, J = 7.4, 6.0, 1.3 Hz, H2, H15), 6.88 (tq J = 7.2, 5.9, 1.2 Hz, H18), 4.63 (s, H25, 3H). ^{13}C NMR (151 MHz, acetone-d_6, 25 °C) δ (ppm): 200.04 (C22), 159.83 (C5, C12), 157.59 (C6, C11), 157.34 (C1, C16), 156,91 (C21), 152.44 (C17), 138.04 (C19), 137.47 (C3, C14), 136.38 (C9), 127.97 (C2, C15), 126.96 (C23), 124.45 (C4, C13), 123.07 (C7, C10), 122.29 (C18), 117.09 (C24), 111.73(C20), 38.21 (C25). NOEs: H25 with H16, H4 with H7, and H20 with H24. IR (ν_{max}, cm^{-1}): 1739 (m), 1610 (m), 1494 (m), 1251 (w), 1124 (m), 1091 (w), 836 (s), 771 (s), 555 (s). $E_{1/2}$(III/II) (CH_2Cl_2 + 0.1 M TBAH): 0.77 V versus SSCE. UV−vis (CH_2Cl_2): λ_{max}, nm (ε, M^{-1} cm^{-1}) 268 (19 824), 280 (14 742), 320 (19 331), 381 (5217), 498 (3898). ESI-MS (m/z): 529.1 [M − PF_6^-]$^+$. For the NMR assignment we have used the same numbering scheme as for the X-ray structure displayed in Figure 1.

***cis*-[Ru^{II}(CN-Me)(trpy)OH$_2$](PF$_6$)$_2$·H$_2$O, *cis*-7·3.5H$_2$O.** A 17 mg (0.025 mmol) sample of *cis*-**6** and an 8.57 mg sample of $AgNO_3$ were placed in a round-bottom flask together with 15 mL of H_2O. The resulting mixture was refluxed for 3 h in darkness. After this time the reaction was placed in an ice bath, and the AgCl formed was removed by filtration over Celite. Afterward, a 1 mL sample of saturated aqueous solution of NH_4PF_6 was added, and the solvent was removed slowly in a rotary evaporator until precipitation of a brown solid that was filtered, washed with ether and then pentane, and dried under vacuum. Yield: 15 mg (74.9%). [Note that in this synthesis we have observed the formation of approximately 20% of the *trans* isomer.] Anal. Found (Calcd) for $C_{24}H_{22}N_6ORuP_2F_{12}$·3.5$H_2O$: C, 33.79 (34.05); N, 9.90 (9.92); H, 2.73 (3.20). ^{1}H NMR (600 MHz, acetone-d_6/10% D_2O, 25 °C) δ (ppm): 8.84 (d, J = 8.1 Hz, H7, H10), 8.65 (d, J = 8.0 Hz, H4, H13), 8.52 (d, J = 2.3 Hz, H24), 8.44 (t, J = 8.1 Hz, H9), 8.22 (dd, J = 7.4, 0.7 Hz, H1, H16), 8.03 (td, J = 7.8, 1.5 Hz, H3, H14), 7.99 (d, J = 8.3 Hz, H17), 7.88 (d, J = 2.3 Hz, H23), 7.75 (tq, J = 8.2, 7.0, 1.4 Hz, H18), 7.41 (tq, J = 7.5, 5.9, 1.1 Hz, H2, H15), 7.39 (d, J = 5.1 Hz, H20), 6.89 (tq, J = 7.3, 6.1, 1.1 Hz, H19), 4.44 (s, H25, 3H). ^{13}C NMR (151 MHz, acetone-d_6/10% D_2O, 25 °C) δ (ppm): 199.51 (C22), 160.11 (C5, C12), 158.50 (C6, C11), 157.75 (C1, C16), 157.41 (C21), 152.97 (C17), 138.99 (C19), 138.82 (C3, C14), 138.51 (C9), 128.68 (C2, C15), 126.96 (C23), 125.05 (C4, C13), 124.02 (C7, C10), 122.52 (C18), 117.53 (C24), 112.00 (C20), 37.19 (C25). IR (ν_{max}, cm^{-1}): 3660 (w), 3500 (s), 1620 (m), 1610 (w), 1494 (m), 1247 (m), 1024 (m), 835 (s), 763 (s), 555 (s). $E_{1/2}$(IV/II), phosphate buffer pH = 7: 0.44 V versus SSCE. UV−vis phosphate buffer pH = 7: λ_{max}, nm (ε, M^{-1} cm^{-1}) 225 (12 647), 268 (8293), 312 (10 774), 361 (2428), 456 (2098). CH_2Cl_2: 271 (17 275), 314 (21 462), 364 (4996), 464 (4104). ESI-MS (m/z): 513.1 [M − H^+ − 2PF_6^-]$^+$.

Instrumentation and Measurements. Fourier transform IR (FTIR) spectra were taken in a Mattson-Galaxy Satellite FT-IR spectrophotometer containing a MKII Golden Gate Single Reflection ATR system. UV−vis spectroscopy was performed on a Cary 50 Scan (Varian) UV−vis spectrophotometer with 1 cm quartz cells. Cyclic voltammetric (CV) experiments were performed in a IJ-Cambria IH-660 potentiostat using a three electrode cell. Glassy carbon electrodes (3 mm diameter) from BAS were used as working electrode, platinum wire as auxiliary, and SSCE as the reference electrode. Electrochemical experiments were performed under either N_2 or Ar atmosphere with degassed solvents. All $E_{1/2}$ values estimated from cyclic voltammetry were calculated as the average of the oxidative and reductive peak potentials $(E_{pa} + E_{pc})/2$ at a scan rate of 100 mV/s whereas they were directly taken from the maximum of the peak in differential pulse voltammetry experiments. Unless explicitly mentioned the concentration of the complexes was approximately 1 mM. In aqueous solutions the pH was adjusted from 0 to 2 with HCl. Potassium chloride was added to keep a minimum ionic strength of 0.1 M. From pH 2 to 10, 0.1 M phosphate buffers were used, and from pH 10 to 12 diluted, CO_2 free, NaOH. Bulk electrolyses were carried out in a three-compartment cell using carbon felt from SOFACEL as the working electrode.

The ^{1}H NMR spectroscopy was carried out on a a Bruker DPX 200 MHz or a Bruker AVANCE 600 MHz spectrometers. Samples were run in acetone-d_6 or a mixture of acetone-d_6 and D_2O, with internal references (residual solvent protons and/or tetramethylsilane). Elemental analyses were performed using a CHNS-O elemental analyzer EA-1108 from Fisons. ESI-MS experiments were performed on a Navigator LC/MS chromatograph from Thermo Quest Finnigan, using acetonitrile as a mobile phase.

The ^{1}H NMR photoisomerization study on complex *cis*-**7** was performed by dissolving the initial *cis*-**7**:*trans*-**7** 1:4 mixture in d_6-acetone containing 10% of D_2O and irradiating the tube with an 80 W lamp. A first spectrum was registered after 2 h, and the mixture was left to evolve under light for 24 h, after which a final spectrum was registered. For acid−base spectrophotometric titrations, 3−4 × 10^{-5} M buffered aqueous solutions of the complexes were used. The pH of

dx.doi.org/10.1021/ic302863h | Inorg. Chem. 2013, 52, 5077−5087

the different solutions was adjusted by adding small volumes (approximately 10 μL) of 4 M NaOH in order to produce a negligible overall volume change. Redox spectrophotometric titrations were performed by sequential addition of a $(NH_4)_2[Ce^{IV}(NO_3)_6]$ 0.1 M solution in HCl to an aqueous solution of the complex.

X-ray Structure Determination. Measurements of the crystals were performed on a Bruker Smart Apex CCD diffractometer using graphite-monochromated Mo Kα radiation (λ = 0.710 73 Å) from an X-ray tube and examined using the following software: data collection, Smart V.5.631 (BrukerAXS 1997-02); data reduction, Saint+ Version 6.36A (Bruker AXS 2001); absorption correction, SADABS version 2.10 (Bruker AXS 2001); and structure solution and refinement, SHELXTL Version 6.14 (Bruker AXS 2000−2003). The crystallographic data as well as details of the structure solution and refinement procedures are reported in Table 1. Data were deposited with the CCDC for *trans,fac*-**3**, *trans,fac*-**4**, and *cis*-**6**. These data can be obtained free of charge from The Cambridge Crystallographic Data Centre via www.ccdc.cam.uk/data_request/cif.

Catalytic Studies. Experiments have been performed in anhydrous dichloromethane at room temperature. In a typical run, Ru catalyst (0.5 mM), alkene (50 mM), and $PhI(OAc)_2$ (100 mM) were stirred at room temperature in dichloromethane (2.5 mL) for 24 h. After the addition of biphenyl (15 mM) as an internal standard, an aliquot was taken for gas chromatography (GC) analysis. The oxidized products were analyzed in a Shimadzu GC-17A gas chromatography apparatus with a TRA-5 column (30 m × 0.25 mm diameter) incorporating a flame ionization detector. GC conditions: initial temperature, 80 °C for 10 min; ramp rate, 10 °C min^{-1}; final temperature, 220 °C; injection temperature, 220 °C; detector temperature, 250 °C; carrier gas, He at 25 mL min^{-1}. All catalytic oxidations were carried out under a N_2 atmosphere.

■ ASSOCIATED CONTENT

Supporting Information

Additional details, figures, and tables. Crystallographic data in CIF format. This material is available free of charge via the Internet at http://pubs.acs.org.

■ AUTHOR INFORMATION

Corresponding Author

*E-mail: montse.rodriguez@udg.edu (M.R.).

Notes

The authors declare no competing financial interest.

■ ACKNOWLEDGMENTS

This research has been financed by MINECO of Spain through Projects CTQ2010-21532-C02-01, CTQ2012-32436, and CTQ2009-08328. Johnson & Matthey LTD are acknowledged for a $RuCl_3 \cdot nH_2O$ loan. M.D. thanks AECID (MAEC) of Spain for the allocation of a MAEC-AECID grant.

■ REFERENCES

(1) (a) Arduengo, A. J.; Harlow, R. L.; Kline, M. *J. Am. Chem. Soc.* **1991**, *113*, 361−365. (b) Herrmann, W.; Kocher, C. *Angew. Chem., Int. Ed.* **1997**, *36*, 2162−2187. (c) Arduengo, A. J. *Acc. Chem. Res.* **1999**, *32*, 913. (d) Herrmann, W. A. *Angew. Chem., Int. Ed.* **2002**, *41*, 1290−1309.

(2) (a) Öfele, K. *J. Organomet. Chem.* **1968**, *12*, 42−43. (b) Wanzlick, H. W.; Schönherr, H. J. *Angew. Chem., Int. Ed.* **1968**, *7*, 141−142. (c) Herrmann, W. A.; Kohl, F. J.; Schwartz, J. In *Synthetic Methods of Organometallic and Inorganic Chemistry*; Herrmann, W. A., Ed.; Georg Thieme Verlag: Stuttgart, 2000; Vol. *9*. (d) Bourissou, D.; Guerret, O.; Gabbai, F. P.; Bertrand, G. *Chem. Rev.* **2000**, *100*, 39−92. (e) Weskamp, T.; Bohm, V. P. W.; Herrmann, W. A. *J. Organomet. Chem.* **2000**, *600*, 12−22. (f) Jafarpour, L.; Nolan, S. P. *J. Organomet. Chem* **2001**, *617*−*618*, 17−27. (g) Jafarpour, L.; Nolan, S. P. *Adv. Organomet. Chem.* **2001**, *46*, 181−222. (h) Herrmann, W. A.; Weskamp, T.; Bohm, V. P. W. *Adv. Organomet. Chem.* **2002**, *48*, 1−69. (i) Dioumaev, V. K.; Bullock, R. M. *Nature* **2003**, *424*, 530−532. (j) McGuinness, D. S.; Gibson, V. C.; Vass, D. F.; Steed, J. W. *J. Am. Chem. Soc.* **2003**, *125*, 12716−12717. (k) Hu, X.; Castro-Rodriguez, L.; Meyer, K. *J. Am. Chem. Soc.* **2003**, *125*, 12237−12245. (l) Diggle, R. A.; Macgregor, S. A.; Whittlesey, M. K. *Organometallics* **2004**, *23*, 1857−1865.

(3) (a) Peris, E.; Loch, J. A.; Mata, J.; Crabtree, R. H. *Chem. Commun.* **2001**, 201−202. (b) Briot, A.; Bujard, M.; Gouverneur, V.; Nolan, S. P.; Mioskowski, C. *Org. Lett.* **2000**, *2*, 1517−1519.

(4) (a) Duan, W. L.; Shi, M.; Rong, G. B. *Chem. Commun.* **2003**, 2916−2917. (b) Clavier, H.; Coutable, L.; Toupet, L.; Guillemin, J. C.; Mauduit, M. *J. Organomet. Chem.* **2005**, *690*, 5237−5254. (c) Arnold, P. L.; Pearson, S. *Coord. Chem. Rev.* **2007**, *251*, 596−609. (d) Pugh, D.; Danopoulos, A. *Coord. Chem. Rev.* **2007**, *251*, 610−641. (e) Ogle, J. W.; Miller, S. A. *Chem. Commun.* **2009**, 5728−5730. (f) Dragutan, V.; Dragutan, I.; Delaude, I.; Demonceau, A. *Coord. Chem. Rev.* **2007**, *251*, 765−794. (g) Herrmann, W. A.; Frey, G. D.; Herdtweck, E.; Steinbeck, M. *Adv. Synth. Catal.* **2007**, *349*, 1677−1691. (h) Ragone, F.; Poater, A.; Cavallo, L. *J. Am. Chem. Soc.* **2010**, *132*, 4249−4258.

(5) (a) Carmona, D.; Cativiela, C.; Elipe, S.; Lahoz, F. J.; Lamata, M. P.; Pilar, M.; Deviu, M. L. R.; Oro, L. A.; Vega, C.; Viguri, F. *Chem. Commun.* **1997**, 2351−2352. (b) Fung, W. H.; Yu, W. Y.; Che, C.-M. *J. Org. Chem.* **1998**, *63*, 7715−7726. (c) Hua, X.; Shang, M.; Lappin, A. G. *Inorg. Chem.* **1997**, *36*, 3735−3740. (d) Seok, W. K.; Son, Y. J.; Moon, S. W.; Lee, H. N. B. *Bull. Korean Chem. Soc.* **1998**, *19*, 1084−1090. (e) Che, C. M.; Cheng, K. W.; Chan, M. C. W.; Lau, T. C.; Mak, C. K. *J. Org. Chem.* **2000**, *65*, 7996−8000. (f) Lau, T. C.; Che, C. M.; Lee, W. O.; Poonl, C. K. *J. Chem. Soc., Chem. Commun.* **1988**, 1406−1407.

(6) (a) Sheldon, R. A.; Kochi, J. K. *Metal-Catalyzed Oxidations of Organic Compounds*; Academic Press: New York, 1981. (b) Hill, C. L. In *Advances in Oxygenated Processes*; Baumstark, A.L., Ed.; JAI Press Inc.: London, 1988; Vol. *1*. (c) Hudlicky, M. *Oxidations in Organic Chemistry*; ACS Monograph Series; American Chemical Society: Washington, DC, 1990.

(7) Masllorens, E.; Rodríguez, M.; Romero, I.; Roglans, A.; Parella, T.; Benet-Buchholz, J.; Poyatos, M.; Llobet, A. *J. Am. Chem. Soc.* **2006**, *128*, 5306−5307.

(8) Dakkach, M.; Fontrodona, X.; Parella, T.; Atlamsani, A.; Romero, I.; Rodríguez, M. *Adv. Synth. Catal.* **2011**, *353*, 231−238.

(9) (a) Concepcion, J. J.; Jurss, J. W.; Templeton, J. L.; Meyer, T. J. *J. Am. Chem. Soc.* **2008**, *130*, 16462−16463. (b) Gerli, A.; Reedijk, J.; Lakin, M. T.; Spek, A. L. *Inorg. Chem.* **1995**, *34*, 1836−1843. (c) Hua, X.; Shang, M.; Lappin, G. *Inorg. Chem.* **1997**, *36*, 3735−3740.

(10) (a) Evans, I. P.; Spencer, A.; Wilkinson, J. *J. Chem. Soc., Dalton Trans.* **1973**, *2*, 204−209. (b) Alessio, E.; Mestroni, G.; Nardin, G.; Attia, W. M.; Calligaris, M.; Sava, G.; Zorzet, S. *Inorg. Chem.* **1988**, *27*, 4099−4106. (c) Alessio, E. *Chem. Rev.* **2004**, *104*, 4203−4242.

(11) Sullivan, B. P.; Calvert, J. M.; Meyer, T. J. *Inorg. Chem.* **1980**, *19*, 1404−1407.

(12) (a) Mola, J.; Romero, I.; Rodríguez, M.; Bozoglian, F.; Poater, A.; Solà, M.; Parella, T.; Benet-Buchholz, J.; Fontrodona, X.; Llobet, A. *Inorg. Chem.* **2007**, *46*, 10707−10716. (b) Mola, J.; Rodríguez, M.; Romero, I.; Llobet, A.; Parella, T.; Poater, A.; Duran, M.; Solà, M.; Benet-Buchholz, J. *Inorg. Chem.* **2006**, *45*, 10520−10529. (c) Sala, X.; Poater, A.; von Zelewsky, A.; Parella, T.; Fontrodona, X.; Romero, I.; Solà, M.; Rodríguez, M.; Llobet, A. *Inorg. Chem.* **2008**, *47*, 8016−8024.

(13) Dakkach, M.; López, M. I.; Romero, I.; Rodríguez, M.; Atlamsani, A.; Parella, T.; Fontrodona, X.; Llobet, A. *Inorg. Chem.* **2010**, *49*, 7072−7079.

(14) (a) Hecker, C. R.; Fanwick, P. E.; McMillin, D. R. *Inorg. Chem.* **1991**, *30*, 659−666. (b) Suen, H.-F.; Wilson, S. W.; Pomerantz, M.; Walsh, J. L. *Inorg. Chem.* **1989**, *28*, 786−791. (c) Bonnet, S.; Schofield, E.; Collin, J.-P.; Sauvage, J.-P *Dalton Trans.* **2003**, 4654−4662. (d) Bonnet, S.; Schofield, E.; Collin, J.-P.; Sauvage, J.-P. *Inorg. Chem.* **2004**, *43*, 8346−8354.

(15) (a) Romero, I.; Rodríguez, M.; Llobet, A.; Collomb-Dunand-Sauthier, M.-N.; Deronzier, A.; Parella, T.; Stoeckli-Evans, H. *J. Chem.*

Soc., Dalton Trans. **2000**, 1689−1694. (b) Sokolov, M.; Umakoshi, K.; Sasaki, Y. *Inorg. Chem.* **2002**, *41*, 6237−6243. (c) Fukui, S.; Kajihara, A.; Hirano, T.; Sato, F.; Suzuki, N.; Nagao, H. *Inorg. Chem.* **2011**, *50*, 4713−4724. (d) Mola, J.; Dinoi, C.; Sala, X.; Rodríguez, M.; Romero, I.; Parella, T.; Fontrodona, X.; Llobet, A. *Dalton Trans.* **2011**, 3640−3646. (e) Fukui, S.; Suzuki, N.; Wada, T.; Tanaka, K.; Nagao, H. *Organometallics* **2010**, *29*, 1534−1536.

(16) (a) Polam, J. R.; Porter, L. C. *J. Coord. Chem.* **1993**, *29*, 109−119. (b) Akita, M.; Takahashi, Y.; Hikichi, S.; Moro-oka, Y. *Inorg. Chem.* **2001**, *40*, 169−172. (c) Serrano, I.; Rodríguez, M.; Romero, I.; Llobet, A.; Parella, T.; Campelo, J. M.; Luna, D.; Marinas, J. M.; Benet-Buchholz, J. *Inorg. Chem.* **2006**, *45*, 2644−2651.

(17) (a) Balzani, V.; Juris, A.; Venturi, M. *Chem. Rev.* **1996**, *96*, 759−833. (b) Haga, M.; Dodsworth, E. S.; Lever, A. B. P. *Inorg. Chem.* **1986**, *25*, 447−453. (c) Takeuchi, K. J.; Thompson, M. S.; Pipes, D. W.; Meyer, T. J. *Inorg. Chem.* **1984**, *23*, 1845−1851.

(18) Baitalik, S.; Flörke, U.; Nag, K. *Inorg. Chem.* **1999**, *38*, 3296−3308.

(19) (a) Passaniti, P.; Browne, W. R.; Lynch, F. C.; Hughes, D.; Nieuwenhuyzen, M.; James, P.; Maestry, M.; Vos, J. G. *J. Chem. Soc., Dalton Trans.* **2002**, 1740−1746. (b) Bell-Loncella, E. T.; Bessel, C. A. *Inorg. Chim. Acta* **2000**, *303*, 199−205. (c) Llanguri, R.; Morris, J. J.; Stanley, W. C.; Bell-Loncella, E. T.; Turner, M.; Boyko, W. J.; Bessel, C. A. *Inorg. Chim. Acta* **2001**, *315*, 53−65.

(20) Rodríguez, M.; Romero, I.; Llobet, A.; Deronzier, A.; Biner, M.; Parella, T.; Stoeckli-Evans, H. *Inorg. Chem.* **2001**, *40*, 4150−4156.

(21) (a) Binstead, R. A.; Meyer, T. J. *J. Am. Chem. Soc.* **1987**, *109*, 3287−3297. (b) Kubow, S. A.; Marmion, M. E.; Takeuchi, K. J. *Inorg. Chem.* **1988**, *27*, 2761−2767. (c) Che, C. M.; Lai, T. F.; Wong, K. Y. *Inorg. Chem.* **1987**, *26*, 2289−2299.

(22) (a) Dobson, J. C.; Meyer, T. J. *Inorg. Chem.* **1988**, *27*, 3283−3291. (b) Llobet, A.; Doppelt, P.; Meyer, T. J. *Inorg. Chem.* **1988**, *27*, 514−520. (c) Cheng, W. C.; Yu, W. Y.; Cheung, K. K.; Che, C. M. *J. Chem. Soc., Dalton Trans.* **1994**, 57−62.

(23) (a) Lever, A. B. P. *Inorg. Chem.* **1990**, *29*, 1271−1285. (b) Dovletoglou, A.; Adeyemi, S. A.; Meyer, T. J. *Inorg. Chem.* **1996**, *35*, 4120−4127.

(24) Vaquer, L.; Miró, P.; Sala, X.; Bozoglian, F.; Masllorens, E.; Benet-Buchholz, J.; Fontrodona, X.; Parella, T.; Romero, I.; Roglans, A.; Rodríguez, M.; Bo, C.; Llobet, A. *ChemPlusChem* **2013**, *78*, 235−243.

(25) Barf, G. A.; Sheldon, R. A. *J. Mol. Catal. A: Chem.* **1995**, *98*, 143−146.

(26) Koola, J. D.; Kochi, J. K. *Inorg. Chem.* **1987**, *26*, 908−916.

(27) Serrano, I.; Sala, X.; Plantalech, E.; Rodríguez, M.; Romero, I.; Jansat, S.; Gómez, M.; Parella, T.; Stoeckli-Evans, H.; Solans, X.; Font-Bardia, M.; Vidjayacoumar, B.; Llobet, A. *Inorg. Chem.* **2007**, *46*, 5381−5389.

(28) (a) Mägerlein, W.; Dreisbach, C.; Hugl, H.; Kin Tse, M.; Klawonn, M.; Bhor, S.; Beller, M. *Catal. Today* **2007**, *121*, 140−150. (b) Terry, T. J.; Stack, T. D. *J. Am. Chem. Soc.* **2008**, *130*, 4945−4953.

(29) Yu, X.-Q.; Huang, J.-S.; Che, C.-M. *J. Am. Chem. Soc.* **2000**, *122*, 5337−5342.

(30) (a) Jacobsen, E. N.; Zhang, W.; Güler, M. L. *J. Am. Chem. Soc.* **1991**, *113*, 6703. (b) Cavallo, L.; Jacobsen, H. *J. Org. Chem.* **2003**, *68*, 6202−6207.

(31) Pal, S.; Chan, M. K.; Armstrong, W. H. *J. Am. Chem. Soc.* **1992**, *114*, 6398−6406.

(32) Gründemann, S.; Kovacevic, A.; Albrecht, M.; Faller, J. W.; Crabtree, R. H. *J. Am. Chem. Soc.* **2002**, *124*, 10473−10481.